

**Supplementary Information:**  
**Room-temperature cavity quantum electrodynamics with**  
**strongly-coupled Dicke states**

Jonathan D. Breeze,<sup>1,2,\*</sup> Enrico Salvadori,<sup>3,4,5</sup> Juna  
Sathian,<sup>1</sup> Neil McN. Alford,<sup>1,2</sup> and Christopher W.M. Kay<sup>3,4</sup>

<sup>1</sup>*Department of Materials, Imperial College London,  
Exhibition Road, London, SW7 2AZ, UK.*

<sup>2</sup>*London Centre for Nanotechnology, Imperial College London,  
Exhibition Road, London, SW7 2AZ, UK.*

<sup>3</sup>*Institute of Structural & Molecular Biology,  
University College London, Gower Street, London, WC1E 8BT, UK.*

<sup>4</sup>*London Centre for Nanotechnology, 17-19 Gordon Street, London, WC1H 0AH, UK.*

<sup>5</sup>*School of Biological and Chemical Sciences,  
Queen Mary University of London, Mile End Road, London, E1 4NS, UK.*

---

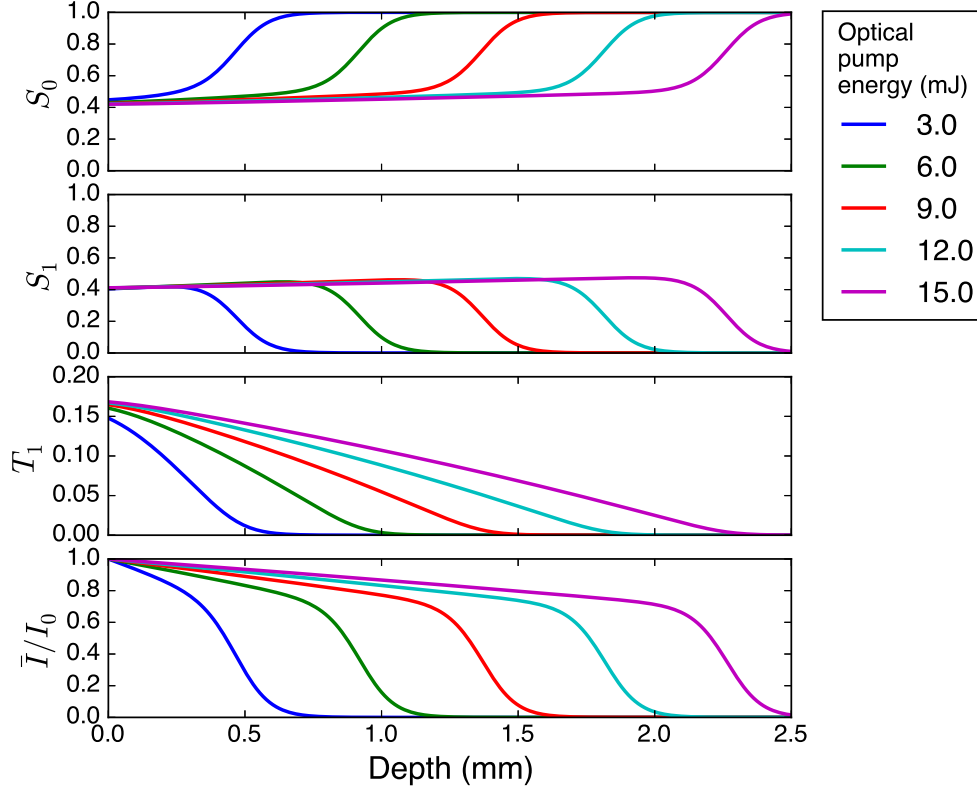
\* jonathan.breeze@imperial.ac.uk

## Penetration of optical pulses into pentacene:*p*-terphenyl crystal

Modelling the penetration of nanosecond optical pulses into a slab of pentacene-doped *p*-terphenyl followed the procedure outlined by Takeda [1], implementing a finite-difference time-domain technique to solve a coupled system of rate equations for the singlet and triplet state densities as a function of depth and a spatial differential equation for the optical beam irradiance. The optical parametric oscillator (OPO) used in this study emitted pulses of duration 5.5 ns at a wavelength of 592 nm with a (gaussian profile) spot diameter of 4 mm. The profile densities of the ground-state singlet, excited-state singlet, triplet state and the normalized optical pump irradiance for increasing optical pulse energies are shown in Fig. 1. For a pulse energy of 15 mJ, a penetration depth of  $\sim 2.5$  mm was calculated for a 0.053% pentacene doped sample. The pentacene concentration places a limit on the thickness (and size) of the pentacene:*p*-terphenyl crystal given the available means of optical pumping. For our OPO with maximum pulse energy of 15 mJ, a cylindrical crystal with diameter 3 mm is sufficient for  $\sim 10\%$  of the pentacene molecules to be excited into the triplet state, yielding an inversion of  $\sim 10^{15}$  between the  $|X\rangle$  and  $|Z\rangle$  sub-levels. Importantly, for a crystal with given pentacene dopant concentration of a prescribed thickness, the triplet yield is a linear function of the laser energy when the penetration depth is less than crystal thickness. Although the number of triplets excited is crudely estimated, the linearity allows the  $\sqrt{N}$  dependence of the ensemble spin-photon coupling  $g_e$  to be inferred by varying the OPO pulse energy. Furthermore, the linearity permits a comparison of estimates of the number of participating spins  $N$  from the numerical modelling and those extracted from the observed normal mode splitting.

### Cavity design

To optimize a cavity for strong-coupling, the ‘cooperativity’  $C = g_e^2/\kappa_s\kappa_c$  is a good figure of merit, yet by no means the criterion for strong-coupling, which is  $g_e \gg \kappa_c, \kappa_s$ , where  $g_e$  is the ensemble spin-photon coupling,  $\kappa_s$  and  $\kappa_c$  are the decay rates for the spin and cavity modes respectively. The ensemble spin-photon coupling  $g_e$  for  $N$  spins situated at the magnetic field maximum is given by  $g_e = g_s\sqrt{N} = \gamma\sqrt{\mu_0\hbar\omega_c N/2V_m}$ , where  $\mu_0$  is the permeability of free-space,  $\hbar$  is the reduced Planck constant,  $\omega_c$  is the resonant frequency



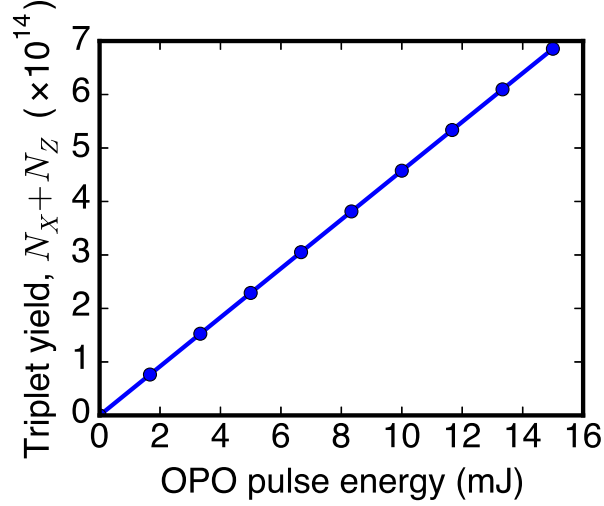
**Supplementary Figure 1. State density and normalized irradiance depth profiles for pulses with increasing energies.** Optical pulses have duration 5.5 ns and energies in the range 3-15 mJ. Graphs are (from top to bottom) ground singlet state  $S_0$  density, excited singlet state  $S_1$  density, spin-triplet state  $T_1$  density, normalized optical pulse irradiance  $\bar{I}/I_0$ . The pentacene concentration is 0.053%. The penetration depth increases linearly as a function of optical pump pulse energy.

of the cavity and  $V_m$  is the magnetic mode volume. The magnetic mode volume,  $V_m$  is calculated as the ratio of the stored magnetic energy within the cavity,  $\frac{1}{2}\mu_0 \int_V |\mathbf{H}(\mathbf{r})|^2 dV$  to the maximum magnetic field energy density,  $\frac{1}{2}\mu_0 |\mathbf{H}(\mathbf{r})|^2$ . Factoring out parameters that are independent of the cavity, like the number of spins  $N$  and the spin decoherence rate  $\kappa_s$ , reduces the ‘cavity cooperativity’ to

$$C_{\text{cav}} \propto \frac{g_s^2}{\kappa_c} \propto \frac{\omega_c}{\kappa_c V_m} \propto \frac{Q}{V_m},$$

which is proportional to the Purcell factor [2] for a given frequency  $\omega_c$ :

$$F_m = \frac{2\pi c^3}{\omega_c^3} \cdot \frac{Q}{V_m}.$$

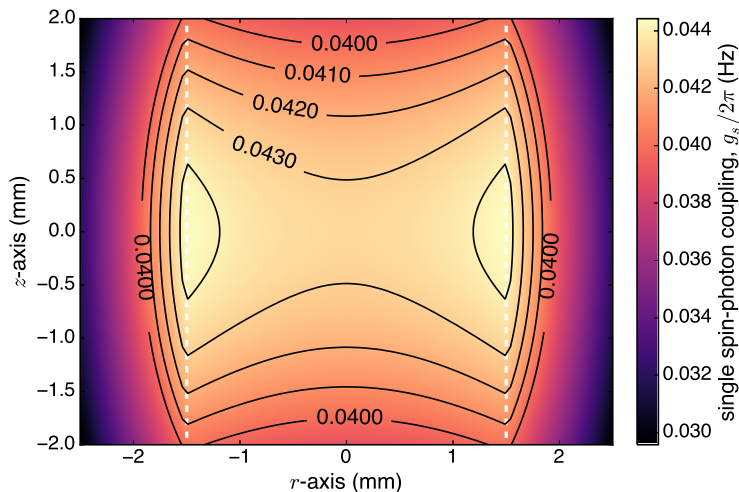


**Supplementary Figure 2. Spin-triplet yield as a function of optical pump pulse energy.**

A pentacene-doped *p*-terphenyl crystal of thickness 3 mm and pentacene concentration 0.053% is excited by optical pump pulses of duration 5.5 ns and increasing energy. The OPO spot size diameter 4 mm.

Optimizing the Purcell factor is therefore a sound strategy for maximising the degree of strong-coupling. The cavity was modelled using a quasi-analytical radial mode-matching technique [3]. A hollow cylinder of single-crystal strontium titanate ( $\text{SrTiO}_3$ , STO) with outer diameter 10 mm, inner diameter 3 mm and height 11 mm was placed upon a cylindrical single-crystal sapphire ( $\text{Al}_2\text{O}_3$ ) support (diameter 10 mm, height 6 mm). The dielectric stack was placed upon the floor of a cylindrical oxygen-free copper cavity with fixed diameter of 36 mm and a mechanically adjustable height of 18-24 mm. The pentacene *p*-terphenyl was housed inside the STO cylinder. The relative permittivity of STO at room temperature is  $\epsilon_r = 318$  and that of sapphire is  $\epsilon_r = 9.3$ . The unloaded  $Q$ -factor is the reciprocal of the sum of the losses within the cavity, such as ohmic losses in cavity walls and dielectric losses within the dielectric resonator. The pentacene-doped *p*-terphenyl gain medium has low dielectric loss and low electric filling factor so its contribution to losses is negligible. The STO and sapphire had loss tangents of  $9 \times 10^{-5}$  and  $2 \times 10^{-6}$  at 1.45 GHz respectively. The surface resistance of the copper shield was 10 m $\Omega$ . The fundamental  $\text{TE}_{01\delta}$  mode had a frequency of  $\approx 1.45$  GHz, an unloaded  $Q$ -factor of 10,200 and a magnetic mode volume  $V_m$  of 0.25 cm<sup>3</sup>.

The magnetic field  $\mathbf{H}(\mathbf{r})$  within the cavity can be directly mapped onto to the coupling strength for an individual spin to a vacuum cavity photon,  $g_{rms}(\mathbf{r}) = \mu_0\gamma H(\mathbf{r})_{vac}$ , where  $\gamma$  is the electron gyromagnetic ratio,  $\mu_0$  is the permeability of free-space and the vacuum magnetic field in the cavity is given by  $H(\mathbf{r})_{vac} = \sqrt{\hbar\omega_c/2\mu_0 \int_V |\mathbf{H}(\mathbf{r})|^2 dV} \cdot |\mathbf{H}(\mathbf{r})|$ . The single spin-photon coupling strength is shown in Fig. 3 for the region of the pentacene *p*-terphenyl illuminated by the optical pulse. Over the central portion  $|r| < 1.5$  mm,  $|z| < 2$  mm, the spin-photon coupling is  $g_s/2\pi = 0.042 \pm 0.002$  Hz.



**Supplementary Figure 3. Single spin-photon coupling strength distribution within pentacene-doped medium.** The spin-photon coupling  $g_s$  for a single spin throughout the portion of the pentacene:*p*-terphenyl crystal illuminated by the optical pump pulse. Over the central portion  $|r| < 1.5$  mm,  $|z| < 2$  mm, the spin-photon coupling is  $g_s/2\pi = 0.042 \pm 0.002$  Hz.

### Master equations: decoherence and thermal noise

The time derivative of the expectation value of an operator  $\hat{O}$  can be written [4]:

$$\frac{d}{dt} \langle \hat{O} \rangle = \text{tr}(\mathcal{O}\dot{\rho}) \quad (1)$$

where  $H$  is the Tavis-Cummings Hamiltonian:

$$H = \hbar\omega_c a^\dagger a + \frac{1}{2}\hbar\omega_s \sum_j \sigma_j^z + \hbar g_s \sum_j (\sigma_j^+ a + a^\dagger \sigma_j^-), \quad (2)$$

and  $\rho$  is the reduced spin-photon density matrix, given by  $\dot{\rho} = (i\hbar)^{-1} [H, \rho] + \mathcal{L}[\rho]$ , where  $\mathcal{L}[\rho]$  is the Liouvillian, which accounts for the dissipative processes of cavity loss, spin-lattice relaxation and spin dephasing.

$$\mathcal{L}[\rho] = \mathcal{L}_{\text{cavity}}[\rho] + \mathcal{L}_{\text{spin-lattice}}[\rho] + \mathcal{L}_{\text{dephasing}}[\rho].$$

Spontaneous emission can be neglected since it is so small at microwave frequencies. Each component of the Liouvillian is given by:

$$\mathcal{L}_{\text{cavity}}[\rho] = \frac{\kappa_c}{2} \mathcal{D}[a]\rho \quad (3)$$

$$\mathcal{L}_{\text{spin-lattice}}[\rho] = \frac{\gamma}{2} \sum_{j=1}^N (\mathcal{D}[\sigma_j^-]\rho + \mathcal{D}[\sigma_j^+]\rho) \quad (4)$$

$$\mathcal{L}_{\text{dephasing}}[\rho] = \frac{\kappa_s}{2} \sum_{j=1}^N \mathcal{D}[\sigma_j^z]\rho \quad (5)$$

where  $\mathcal{D}[\mathcal{O}]\rho = 2\mathcal{O}\rho\mathcal{O}^\dagger - \mathcal{O}^\dagger\mathcal{O}\rho - \rho\mathcal{O}^\dagger\mathcal{O}$  is the Lindblad superoperator,  $\kappa_c = \omega_c/Q$  is the cavity photon decay rate,  $\gamma$  is the spin-lattice relaxation rate and  $\kappa_s = 2/T_2$  is the spin dephasing rate. An exact expression for the rate of change of the expectation value for the cavity photon number  $\langle n \rangle = \langle a^\dagger a \rangle$  can be derived from Eq. 1:

$$\frac{d}{dt} \langle a^\dagger a \rangle = -\kappa_c \langle a^\dagger a \rangle + \kappa_c \bar{n} + igN (\langle \sigma_1^+ a \rangle - \langle a^\dagger \sigma_1^- \rangle) \quad (6)$$

where  $\bar{n} = 1/(e^{\hbar\omega_c/kT} - 1)$  is the average thermal photon population in the cavity. The average photon number  $\langle n \rangle = \langle a^\dagger a \rangle$  couples to the spins through the last term, the spin-photon coherence  $\langle \sigma_1^+ a \rangle = \langle a^\dagger \sigma_1^- \rangle^*$ . As one would expect the photon number decays with rate  $\kappa_c$ . The spin-photon coherence rate is

$$\frac{d}{dt} \langle \sigma_1^+ a \rangle = - \left( \frac{\kappa_c}{2} + \frac{\gamma}{2} + \frac{\kappa_s}{2} + i\Delta \right) \langle \sigma_1^+ a \rangle - ig_s \left[ \frac{\langle \sigma_1^z \rangle + 1}{2} + (N-1) \langle \sigma_1^+ \sigma_2^- \rangle + \langle a^\dagger a \rangle \langle \sigma_1^z \rangle \right] \quad (7)$$

where third order cumulants and higher have been neglected and  $\Delta = \omega_c - \omega_s$  is the frequency detuning parameter. Note that since the system is not being driven or pumped by coherent fields, there is no well-defined phase so that we can take  $\langle a \rangle = \langle a^\dagger \rangle = \langle \sigma_1^\pm \rangle = 0$ . The rate of change of the inversion  $\langle \sigma_1^z \rangle$  is also exact:

$$\frac{d}{dt} \langle \sigma_1^z \rangle = -\gamma \langle \sigma_1^z \rangle - 2ig_s (\langle \sigma_1^+ a \rangle - \langle a^\dagger \sigma_1^- \rangle) \quad (8)$$

and finally, the set of equations is closed by the spin-spin correlation:

$$\frac{d}{dt} \langle \sigma_1^+ \sigma_2^- \rangle = -(\gamma + \kappa_s) \langle \sigma_1^+ \sigma_2^- \rangle + ig_s \langle \sigma_1^z \rangle (\langle \sigma_1^+ a \rangle - \langle a^\dagger \sigma_1^- \rangle), \quad (9)$$

where again third-order terms have been neglected.

In terms of normalized collective spin operators:

$$\tilde{S}^\pm = \frac{1}{\sqrt{N}} \sum_i^N \sigma_i^\pm, \quad \tilde{S}^z = \frac{1}{N} \sum_i^N \sigma_i^z = \frac{1}{N} S^z,$$

the closed set of coupled equations become:

$$\begin{aligned} \frac{d}{dt} \langle a^\dagger a \rangle &= -\kappa_c \langle a^\dagger a \rangle + \kappa_c \bar{n} + ig_e (\langle \tilde{S}^+ a \rangle - \langle a^\dagger \tilde{S}^- \rangle) \\ \frac{d}{dt} \langle \tilde{S}^+ a \rangle &= -\left( \frac{\kappa_c}{2} + \frac{\gamma}{2} + \frac{\kappa_s}{2} + i\Delta \right) \langle \tilde{S}^+ a \rangle - ig_e \left[ \frac{\langle \tilde{S}^z \rangle + 1}{2} + \left( 1 - \frac{1}{N} \right) \langle \tilde{S}^+ \tilde{S}^- \rangle + \langle a^\dagger a \rangle \langle \tilde{S}^z \rangle \right] \\ \frac{d}{dt} \langle \tilde{S}^z \rangle &= -\gamma \langle \tilde{S}^z \rangle - 2ig_e \frac{1}{N} (\langle \tilde{S}^+ a \rangle - \langle a^\dagger \tilde{S}^- \rangle) \\ \frac{d}{dt} \langle \tilde{S}^+ \tilde{S}^- \rangle &= -(\gamma + \kappa_s) \langle \tilde{S}^+ \tilde{S}^- \rangle + ig_e \langle \tilde{S}^z \rangle (\langle \tilde{S}^+ a \rangle - \langle a^\dagger \tilde{S}^- \rangle) \end{aligned}$$

where  $g_e = g_s \sqrt{N}$  is the collective spin-photon coupling. Given initial conditions  $\langle a^\dagger a \rangle = \bar{n} \sim 4.3 \times 10^3$ ,  $\langle \tilde{S}^+ a \rangle = 0$ ,  $\langle \tilde{S}^z \rangle = 0.8$ ,  $\langle \tilde{S}^+ \tilde{S}^- \rangle = 0$  and suitable values for the single-spin photon coupling  $g_s$ , cavity decay rate  $\kappa_c$ , spin decoherence rate  $\kappa_s$  and number of spins  $N$ , the set of equations can be integrated in time, using for example the Runge-Kutta method, to reveal the dynamics of the expectation values.

### Pentacene:*p*-terphenyl crystal growth

Commercially available pentacene powder (TCI Europe NV) was vacuum purified and *p*-terphenyl commercial powder (Alfa Aesar, 99%+, AL4833) was zone-refined. 0.053% mol/mol pentacene in *p*-terphenyl powder was prepared and sealed in a 3 mm inner diameter surface modified quartz ampoule with vacuum level of around  $10^{-3}$  mbar. A sharp tip was made at one of end of the ampoule for self-seeding. The wall surfaces of the ampoule were coated with 1H,1H,2H,2H-perfluorodecyltrichlorosilane (FDTS) and cleaned thoroughly using solvents (acetone, isopropanol and distilled water) in an ultrasonic bath. A zone melting technique was used to grow the pentacene-doped *p*-terphenyl crystal. An in-house furnace's temperature was controlled with a Eurotherm 3216 temperature controller and TE10A power

controller to conduct the zone melting process at a temperature of 200 °C. The melt zone temperature was set at 230 °C. The ampoule was lowered through the furnace at a rate of around 1 mm per hour using a gear motor. Thereafter, the furnace was cooled down at 1 °C per hour to room temperature and the ingot retrieved. Due to the manner of crystal growth (habit), the triclinic  $c$ -plane exists along the ampoule long-axis.

#### SUPPLEMENTARY REFERENCES

- [1] Takeda, K., Takegoshi, K. & Terao, T. Zero-field electron spin resonance and theoretical studies of light penetration into single crystal and polycrystalline material doped with molecules photoexcitable to the triplet state via intersystem crossing. *J. Chem. Phys.* **117**, 4940–4946 (2002).
- [2] Purcell, E. Spontaneous emission probabilities at radio frequencies. *Phys. Rev.* **69**, 681 (1946).
- [3] Kajfez, D. & Guillon, P. *Dielectric Resonators* (Artech House, Inc., 1964), 1st edn.
- [4] Carmichael, H. J. *Statistical Methods in Quantum Optics 1: Master Equations and Fokker-Planck Equations* (Springer, 2003).